Title
Attribution of divergent northern vegetation growth responses to lengthening non-frozen seasons using satellite optical-NIR and microwave remote sensing

Journal
International Journal of Remote Sensing, 35(10)

ISSN
0143-1161

Authors
Kim, Youngwook
Kimball, JS
Zhang, K
et al.

Publication Date
2014-05-19

DOI
10.1080/01431161.2014.915595

International Journal of Remote Sensing, 2014
Vol. 35, No. 10, 3700–3721, http://dx.doi.org/10.1080/01431161.2014.915595

Taylor & Francis
Taylor & Francis Group

Attribution of divergent northern vegetation growth responses to lengthening non-frozen seasons using satellite optical-NIR and microwave remote sensing

Youngwook Kim[a,b]*, J.S. Kimball[a,b], K. Zhang[c], K. Didan[d], I. Velicogna[e], and K.C. McDonald[f,g]

[a]*Flathead Lake Biological Station, The University of Montana, Polson, MT 59860, USA;* [b]*Numerical Terradynamic Simulation Group, The University of Montana, Missoula, MT 59812, USA;* [c]*Department of Organismic and Evolutionary Biology, Harvard University, Cambridge, MA 02138, USA;* [d]*Department of Electrical and Computer Engineering, The University of Arizona, Tucson, AZ 85721, USA;* [e]*Earth System Science, The University of California, Irvine, CA 92697, USA;* [f]*Earth and Atmospheric Sciences, The City College of New York, New York, NY 10031, USA;* [g]*Jet Propulsion Laboratory, California Institute of Technology, Pasadena, CA 91109, USA*

(*Received 17 July 2013; accepted 17 March 2014*)

The non-frozen (NF) season duration strongly influences the northern carbon cycle where frozen (FR) temperatures are a major constraint to biological processes. The landscape freeze-thaw (FT) signal from satellite microwave remote sensing provides a surrogate measure of FR temperature constraints to ecosystem productivity, trace gas exchange, and surface water mobility. We analysed a new global satellite data record of daily landscape FT dynamics derived from temporal classification of overlapping SMMR and SSM/I 37 GHz frequency brightness temperatures (T_b). The FT record was used to quantify regional patterns, annual variability, and trends in the NF season over northern (≥45°N) vegetated land areas. The ecological significance of these changes was evaluated against satellite normalized difference vegetation index (NDVI) anomalies, estimated moisture and temperature constraints to productivity determined from meteorological reanalysis, and atmospheric CO_2 records. The FT record shows a lengthening (2.4 days decade^{-1}; $p < 0.005$) mean annual NF season trend (1979–2010) for the high northern latitudes that is 26% larger than the Northern Hemisphere trend. The NDVI summer growth response to these changes is spatially complex and coincides with local dominance of cold temperature or moisture constraints to productivity. Longer NF seasons are predominantly enhancing productivity in cold temperature-constrained areas, whereas these effects are reduced or reversed in more moisture-constrained areas. Longer NF seasons also increase the atmospheric CO_2 seasonal amplitude by enhancing both regional carbon uptake and emissions. We find that cold temperature constraints to northern growing seasons are relaxing, whereas potential benefits for productivity and carbon sink activity are becoming more dependent on the terrestrial water balance and supply of plant-available moisture needed to meet additional water use demands under a warming climate.

1. Introduction

The high northern latitude (HNL) land areas have experienced greater surface air temperature warming than the global average in recent decades (Liu et al. 2007; Serreze and Francis 2006; Winton 2006). Recent environmental changes attributed to HNL warming include earlier and longer potential growing seasons (Nemani et al. 2003; Kim et al.

*Corresponding author. Email: youngwook.kim@ntsg.umt.edu

2012), vegetation greening (Beck and Goetz 2011; Bunn and Goetz 2006; Hudson and Henry 2009) and productivity increases (Zhang et al. 2008), a northward shift in vegetation biomes (Lucht et al. 2006), and tundra shrub expansion (McManus et al. 2012; Tape et al. 2012). HNL vegetation growth is primarily constrained by seasonal cold temperatures (Nemani et al. 2003; Friedlingstein et al. 2006; Qian, Joseph, and Zeng 2010), but recent reports indicate that widespread drought and wildfire disturbances exacerbated by continued warming have resulted in the frequent occurrences of tree mortality and declines in boreal productivity (Girardin and Mudelsee 2008; Goetz et al. 2005; Peng et al. 2011). Spatially extensive patterns of drought-induced vegetation growth decline have also been reported across the HNL domain (Goetz et al. 2012; Kim et al. 2012; Schaphoff et al. 2006; Zhang et al. 2008), including interior Alaska (Baird, Verbyla, and Hollingsworth 2012; Beck et al. 2011; Verbyla 2008), Canada (Ma et al. 2012; Peng et al. 2011), and Eurasia (Park and Sohn 2010; Piao et al. 2011).

Arctic tundra and boreal forests represent the dominant HNL biomes and cover approximately 25% of the global vegetated land surface (McGuire et al. 2009). Both biomes store a considerable amount of carbon in seasonally frozen (FR) ground that favours soil organic carbon (SOC) accumulation over microbial decomposition. The status of HNL terrestrial carbon sink activity under continued climate warming remains unclear due to uncertainty regarding the potential productivity benefits of lengthening growing seasons and increasing vulnerability of vegetation and SOC stocks to disturbances from drought, wildfire and insects, and increasing SOC decomposition and respiration from permafrost melting (McGuire et al. 1995; Zimov, Schuur, and Chapin 2006; Kimball et al. 2007).

The normalized difference vegetation index (NDVI) derived from satellite optical and near-infrared (NIR) remote sensing has been widely used to document vegetation responses to climate variability and global warming (Lloyd, Bunn, and Berner 2011; Raynolds et al. 2012; Xu et al. 2013). The NDVI is sensitive to canopy photosynthetic activity (Field, Randerson, and Malmström 1995; Huete et al. 2002; Tucker, Townshend, and Goff 1985), and has been commonly used to analyse regional patterns and temporal variability and trends in HNL vegetation growth (Bi et al. 2013; Goetz et al. 2005; Piao et al. 2011). However, seasonal reductions in solar illumination and persistent clouds, smoke, and other atmospheric effects can degrade satellite NDVI retrieval accuracy over many areas, especially at higher latitudes (Alcaraz-Segura et al. 2010; Nagol, Vermote, and Prince 2009; Shuai et al. 2008).

Recently, Kim et al. (2012) developed a consistent global record of daily landscape freeze-thaw (FT) dynamics by temporal change classification of satellite passive microwave brightness temperature retrievals that are relatively insensitive to atmosphere and solar illumination effects (Jones et al. 2010; Kim et al. 2011; Naeimi et al. 2012). The satellite microwave FT signal senses the predominant FR or non-frozen (NF) status of water in surface soil and vegetation canopy layers (Kim et al. 2011; Zhao et al. 2011), and has been linked to FR temperature constraints to vegetation productivity, landscape water mobility, and land-atmosphere carbon exchange over the HNL domain (Kimball et al. 2004; McDonald et al. 2004; Zhang et al. 2011). Kim et al. (2012) applied the satellite FT record and documented significant Northern Hemisphere trends of lengthening NF seasons consistent with recent global warming from 1979 to 2008. The FT results were compared against satellite (MODIS) optical-NIR-derived summer NDVI growth anomalies over a 9 year (2000–2008) record. They showed that longer NF seasons have generally promoted widespread vegetation canopy growth, with the relative benefits

increasing at higher latitudes, and reduced or degraded productivity effects at lower latitudes.

For this investigation we hypothesized that the regional patterns in the HNL canopy growth response to longer NF seasons are dependent on underlying cold temperature or moisture constraints to annual vegetation productivity. A positive canopy growth response to longer NF seasons is expected to occur in cold-temperature-dominant landscapes, whereas in regions where summer moisture supply plays a greater role in limiting vegetation productivity the growth response will be reduced or reversed due to more frequent summer droughts and stronger evaporative demands. Potential moisture and temperature constraints underpinning the regional growth changes were evaluated using ancillary moisture- and temperature-constraint metrics derived from global reanalysis daily surface meteorology records. To verify our hypothesis we analysed a 29 year satellite microwave FT record to quantify NF season variability and trends over the HNL (≥45ºN) domain. We evaluated the ecological significance of these changes by comparing the FT record with an independent and well-calibrated satellite NDVI record in order to clarify the effects of FT-derived NF season variability on vegetation canopy growth for dominant cold temperature- and moisture-constrained areas within the HNL domain. We also compared the FT record with regional atmospheric CO_2 observations to specify how potential growing season changes associated with FT cycle variability are influencing HNL atmospheric CO_2 seasonal cycles.

2. Methods and data

2.1. Satellite microwave FT metrics

We used a global Earth System Data Record of daily landscape freeze–thaw status (FT-ESDR) derived from satellite microwave remote sensing to define FT metrics over all northern (≥45ºN) vegetated land areas (Kim et al. 2011). The FT-ESDR provides a daily (AM and PM) retrieval representing the predominant FR or NF status of the land surface within the satellite sensor field-of-view (approximately 25 km resolution). Overlapping 37 GHz, vertically polarized (V) brightness temperature (T_b) time series from the Scanning Multichannel Microwave Radiometer (SMMR) and Special Sensor Microwave Imager (SSM/I) have been integrated to produce a consistent and continuous long-term daily global FT data record currently extending from 1979 to 2010 (Kim et al. 2013); the FT retrieval is derived on a grid-cell-wise basis using a temporal change classification of daily T_b values in relation to FR and NF T_b reference states using a seasonal threshold algorithm (STA) (Kim et al. 2011). Cross-sensor compatibility between the SMMR and SSM/I has been implemented through pixel-wise adjustment of the SMMR T_b record based on empirical analyses of overlapping SMMR and SSM/I T_b measurements (Kim et al. 2012). The FT-ESDR for this study is gridded to a global cylindrical Equal-Area Scalable Earth grid (EASE-Grid) projection with 25 km grid cell resolution (Brodzik and Knowles 2002). The FT-ESDR encompasses global vegetated land areas where seasonal FR temperatures significantly impact annual vegetation productivity (Kim et al. 2011). Four discrete FT classification levels are provided from daily composite conditions (CO): FR (AM and PM frozen), NF (AM and PM thawed), Transitional (AM FR and PM thawed), and Inverse Transitional (AM thawed and PM FR) statuses. The FT-ESDR showed mean annual FT spatial classification accuracies of 91.4 ±1.05 [inter-annual standard deviation (SD)] and 84.2 ±0.92 [inter-annual SD] percents for respective satellite ascending (PM) and descending (AM) overpasses in

relation to daily surface air temperature records from the global WMO weather station network (Kim et al. 2012). Additional FT-ESDR quality assessment (QA) maps were developed for each annual data record, and provide more spatially explicit data quality information (Kim et al. 2011, 2012).

The FT-ESDR daily CO FT series was used in this investigation to assess HNL regional patterns, annual variability, and temporal trends in the timing and duration of the NF season, FR season, and transitional (TR) frost days for the 1979–2010 period. The NF and FR periods were derived from the daily CO FT record by summing the number of classified NF and FR days, respectively. Similarly, the number of TR days was determined as the sum of classified TR days for each grid cell within the domain. The day of primary seasonal thaw (T_{thaw}) for each cell was determined as the first day for which 12 out of 15 consecutive days (i.e. 80% rule) from January to June were classified as NF (Zhang et al. 2011; Kim et al. 2012; Bi et al. 2013).

2.2. *Satellite NDVI*

The NDVI from satellite (MODIS) optical-NIR remote sensing has been used to investigate the relative benefits of lengthening NF seasons for vegetation growth (Kim et al. 2012). For this investigation, bi-weekly 0.05º× 0.05º (5.6 km) resolution NDVI records provided by the University of Arizona Vegetation Index and Phenology lab (VIP) were used to identify HNL regional patterns and variability in mean summer (JJA) vegetation greenness anomalies over the longest available NDVI data record (1982–2010); the VIP product represents a continuous, well-calibrated global NDVI record derived from multiple overlapping satellite optical-NIR sensors (Didan 2010). The VIP NDVI records for the 1982–1999 period were derived primarily from Advanced Very High Resolution Radiometer (AVHRR) daily surface reflectance measurements. For the period 2000–2010 the VIP record was derived primarily using MODIS (Moderate Resolution Imaging Spectroradiometer) spectral reflectances from the EOS Terra (starting from March 2000) and Aqua (starting from June 2002) satellites. Similar overlapping satellite spectral reflectance data from the SPOT4-VGT (vegetation instrument of the System Pour l'Observation de la Terre 4) sensor were used to bridge the 1999 AVHRR and MODIS records. The AVHRR NDVI was adjusted to the corresponding MODIS NDVI using spectral transformation equations for constructing long-term consistent NDVI records (Miura, Huete, and Yoshioka 2006). For this investigation we selected the VIP record because it represented the longest continuous global NDVI record available (1982–2010 period) with documented data quality information. Other satellite NDVI global data records are also available, including the Global Inventory Modeling and Mapping Studies (GIMMS; Tucker et al. 2005) product; however, regionally dissimilar trends and large discrepancies have been documented between GIMMS and other AVHRR NDVI records within the HNL domain (Alcaraz-Segura et al. 2010; Hall, Masek, and Collatz 2006; McCloy et al. 2005). The GIMMS NDVI record also only extended up to 2006 at the time of this investigation.

Cloudless and snow-free NDVI pixels determined from pixel-wise best data quality (QA) metrics were used for reprojection from the climate modelling grid (CMG) VIP product format to the 25 km global EASE-Grid of the FT-ESDR. We calculated the average summer NDVI conditions for each grid-cell ($NDVI_{JJA}$) by averaging June, July, and August NDVI values. The NDVI retrieval accuracy in spring is relatively more susceptible to degradation from artefacts, including snow cover and cloud effects, which are independent of canopy changes (Dye and Tucker 2003; Suzuki et al. 2011). We therefore used summer NDVI data as a surrogate measure of peak annual vegetation

growth and to investigate how changes in FT status impact productivity in the HNL region as mediated by estimated cold temperature or moisture constraints.

2.3. *Defining primary temperature- and moisture-constrained regions*

A bio-climatological moisture stress index (MSI) and cold temperature stress index (TSI) were produced at 25 km spatial resolution for the 1982–2010 period and HNL domain following Zhang et al. (2008); the TSI and MSI were determined from surface daily minimum air temperature and vapour pressure deficit (VPD) parameters from global reanalysis data and used to define estimated environmental constraints to HNL annual vegetation net primary production (NPP). All daily surface meteorological variables used to define the MSI and TSI were derived from the National Centers for Environmental Prediction and National Center for Atmospheric Research (NNR; Kalnay et al. 1996; Kistler et al. 2001) global reanalysis following Zhang et al. (2008). Despite well-known deficiencies in the NNR product (Kanamitsu et al. 2002), NNR reanalysis data capture the major changes in surface climate anomalies (Simmons et al. 2004) and have been successfully used as meteorological inputs to estimate HNL and global vegetation productivity patterns and environmental trends (Nemani et al. 2003; Kimball, McDonald, and Zhao 2006; Zhang et al. 2008). To minimize influences of known errors in the NNR and other reanalysis data, the 29 year mean TSI and MSI values were used as climatological indicators of dominant cold temperature- and moisture-constrained grid cells, rather than attempting to represent more detailed MSI and TSI temporal trends. NNR reanalysis data at 1.9° (latitude) by 1.875° (longitude) were re-projected to the 25 km global EASE-Grid of the FT-ESDR. Daily VPD was used as a meteorological input for the MSI calculations rather than precipitation, because the atmosphere evaporative demand generally corresponds to soil wetness (Zhang et al. 2010) and large uncertainty in NNR precipitation has been documented (Drobot et al. 2006; Rawlins et al. 2006). Average daily air temperature and atmospheric vapour pressure were used to calculate daily VPD. The TSI was determined from minimum daily air temperature using a photosynthetic response curve that varies with plant functional type defined from a global land-cover classification (Zhang et al. 2008). An MSI value of 1 indicates effective photosynthesis cessation due to extreme moisture constraints to plant growth, whereas a value of 0 indicates that photosynthesis is not constrained by plant-available moisture limitations. The TSI defines the proportional loss of potential NPP due to cold temperatures, where the TSI ranges from 0 to 1 with increasing cold temperature constraints to NPP (Zhang et al. 2008). We calculated annual summer mean TSI (TSI_{JJA}) and MSI (MSI_{JJA}) values for each grid cell within the HNL domain. These climate constraints were used as relative indicators of the moisture and temperature control factors influencing vegetation productivity. Dominant moisture (MSI)- and temperature (TSI)-constrained cells were determined from differences between MSI_{JJA} and TSI_{JJA} averaged over the 1982–2010 period for which VIP NDVI data are available; the resulting dominant moisture- and temperature-constrained cells were assigned as respective positive and negative values of these differences, respectively.

2.4. *NOAA GLOBALVIEW-CO_2*

We used the FT-ESDR as a surrogate indicator of FR temperature constraints to the HNL atmosphere seasonal CO_2 cycle. The FT metrics were compared against atmosphere CO_2 seasonal shape metrics defined from HNL monitoring stations represented by the NOAA

ESRL GLOBALVIEW-CO_2 record (GLOBALVIEW-CO_2 2011). Because seasonal CO_2 cycles are strongly influenced by regional differences between ecosystem net carbon uptake (NPP) and carbon release from soil heterotrophic respiration, biomass burning, and anthropogenic emissions (Patra et al. 2005; Qian, Joseph, and Zeng 2010; Randerson et al. 1997; Sitch et al. 2007), it is necessary to address issues on the sparseness and temporal discontinuity in CO_2 observations when defining atmospheric CO_2 seasonal shape metrics (Vadrevu and Choi 2011; Xueref-Remy et al. 2010). Since the GLOBALVIEW-CO_2 record is derived from the integration of surface, tower, and aircraft measurements by an atmospheric transport model (Masarie and Tans 1995), this record is considered suitable for representing aggregated HNL atmospheric CO_2 variability (Higuchi et al. 2003; Murayama, Taguchi, and Higuchi 2004). The timing of atmospheric CO_2 drawdown by vegetation net photosynthesis in spring (C_{spr}) was computed from the weekly GLOBALVIEW-CO_2 record (>50°N) on an annual basis as the timing (day of year) of the downward 0-ppm crossing of the normalized (weekly – annual mean) atmospheric CO_2 seasonal record (McDonald et al. 2004; Randerson et al. 1999), and coinciding with the HNL growing season initiation (McDonald et al. 2004; Zhang et al. 2008). The annual minimum CO_2 concentration of the normalized seasonal record (C_{min}) was used as a relative measure of net photosynthetic carbon uptake (McDonald et al. 2004; Randerson et al. 1997). The magnitude of the normalized CO_2 concentration at the end of each calendar year (C_{end}) was used as an indicator of net ecosystem carbon release from soil heterotrophic respiration, biomass burning (Yi et al. 2009; Bond-Lamberty et al. 2007), and anthropogenic emissions (Le Quéré et al. 2009). In this study, the HNL aggregated mean annual NF season and T_{thaw} anomalies from the FT-ESDR were compared against the corresponding atmosphere CO_2 seasonal metrics for the 1979–2010 period to investigate the potential impacts of annual variability in the NF season and primary spring thaw timing on the HNL atmospheric CO_2 seasonal cycle.

2.5. Statistical methods

Temporal trend analysis was used to quantify regional trends in NF season and NDVI summer growth changes over the HNL domain and for the 1982–2010 period. Monthly trends of HNL FT metrics derived from the longer (1979–2010) FT-ESDR record were used to examine seasonal changes of individual FT metrics and their relative contributions to the annual FT trends. The temporal trends in FT metrics and $NDVI_{JJA}$ growth anomalies were determined using a non-parametric Theil-Sen slope estimator approach, defined as the median of all pairs of slopes (Sen 1968). This approach is more accurate than simple linear regression when dealing with skewed and heteroscedastic data, and provides similar performance to the simple least squares method for normally distributed data (Akritas, Murphy, and LaValley 1995; Sen 1968). Pre-whitened series removed autocorrelation was used to compute the trends and their significance using the ZYP package in R statistics (Yue, Pilon, and Cavadias 2002) to mitigate autocorrelation effects and avoid trend test failure in the satellite time series (de Beurs and Henebry 2005). This method is insensitive to outliers, which are a challenge to all remote-sensing-based datasets (Alvera-Azcárate et al. 2012). Similar non-parametric approaches have been successfully used for environmental trend studies on a grid-cell-wise basis (Alcaraz-Segura et al. 2010; de Jong et al. 2011; Pouliot, Latifovic, and Olthof 2009).

We first calculated temporal anomalies of the FT metrics, $NDVI_{JJA}$, and atmospheric CO_2 seasonal shape metrics with respect to average values defined from the period of record in case of having non-significant trends over the grid cells. If a significant ($p \leq 0.1$)

trend was determined, the temporal anomalies were derived as differences from the long-term detrended mean. When the trends and correlations were analysed, an outlier detection approach was applied to remove anomalous values with respect to the adjacent time sequence, and largely due to remaining optical-NIR cloud and aerosol contamination, and sensor discontinuity (Alvera-Azcárate et al. 2012). Outliers were identified on a grid-cell-wise basis as values exceeding ±2 times the SD of the long-term mean (Moore 2006) and screened from the analysis. All statistical analyses were evaluated using a 90% ($p \leq 0.1$) minimum threshold of significance.

We evaluated grid-cell-wise temporal correspondence between VIP $NDVI_{JJA}$ and NF season anomalies from the FT-ESDR record over the HNL domain. To evaluate the effects of NF season variability on HNL vegetation canopy growth within dominant temperature (TSI)- and moisture (MSI)-constrained areas we defined the NF period from January to August (NF_{JaAu}), coinciding with the period affecting $NDVI_{JJA}$ (Kim et al. 2012). The Pearson correlation coefficient (r) between $NDVI_{JJA}$ (independent variable) and NF_{JaAu} (dependent variable) anomalies was used to assess the sign and strength of these relationships. Tundra, boreal forest, grassland, and temperate forest biomes within the HNL domain were categorized by a global terrestrial biome map (Olson et al. 2001), and the $NDVI_{JJA}$ and NF_{JaAu} relationships were summarized for these individual biomes.

3. Results

3.1. FT-ESDR QA

The FT-ESDR QA map (Figure 1(*a*)), averaged for the 1979–2010 period, provides a discrete, qualitative indicator of FT product quality for each grid cell within the HNL domain (Kim et al. 2011, 2013). The QA geographical map shows regions of relative high

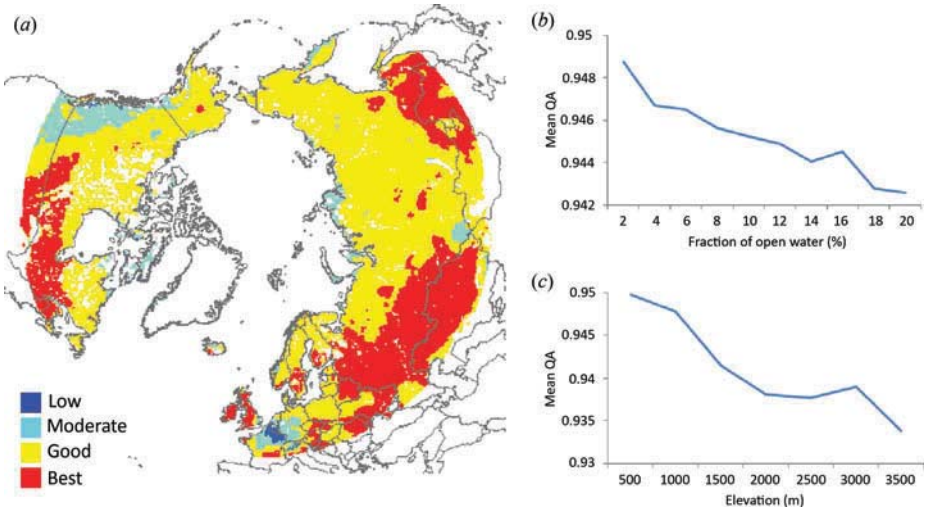

Figure 1. The mean annual FT-ESDR data QA map for the 1979–2010 record and HNL domain, aggregated by relative low (estimated spatial classification accuracy < 70%) to best (estimated accuracy > 90%) quality categories (*a*); the dimensionless QA values range from 0 to 1 for relative low to best quality categories and are responsive to landscape heterogeneity, with generally lower FT-ESDR data quality under higher fractional (% of grid cell) open water cover (*b*) and upper elevations (*c*).

to low product quality in relation to potential negative impacts on FT classification accuracy from temporal gaps in sensor T_b data time series, active precipitation, open water, terrain and land-cover heterogeneity effects, and uncertainty associated with the use of global reanalysis temperature data to define per grid-cell FR and NF T_b reference state thresholds for the STA-based FT classifications. Stepwise linear regression was used to define the independent variables influencing ($R^2 \sim 0.44$) FT classification accuracy and the resulting QA values derived from the SMMR and SSM/I T_b records. The QA values provide a dimensionless relative indicator of FT-ESDR data quality and range from 0 to 1 with increasing quality of the FT classification. The resulting HNL QA map ranges from low (estimated mean annual FT spatial classification accuracy < 70%) to moderate (70% < accuracy < 80%), good (80% < accuracy < 90%), and best (accuracy > 90%) quality categories. The mean proportions of the four QA categories encompass 30.6% (best), 59.5% (good), 9.2% (moderate), and 0.7% (low) of the HNL domain for the 1979–2010 FT-ESDR data record. The mean QA values are generally proportional to regional gradients in open water fraction and elevation over the domain (Figures 1(*b*) and (*c*)), with generally greater QA values at lower elevations and lower open water fractional coverage.

3.2. *FT-ESDR trend analysis*

The HNL FT-ESDR results show a strong latitudinal NF season gradient with shorter NF seasons at more northerly latitudes and a mean annual NF period of 177.6 ± 47.6 [Spatial SD] days over the HNL domain (Figure 2(*a*)). The FT results show a generally longer NF period and larger NF season variability along coastal margins relative to inland areas (Figures 2(*a*) and (*b*)). The FT record also shows a strong, positive HNL trend (2.4 days decade^{-1}; $p < 0.005$) in the mean annual NF period that is largely driven by an NF season increase from March to June (Figure 3); the positive NF days' trend in

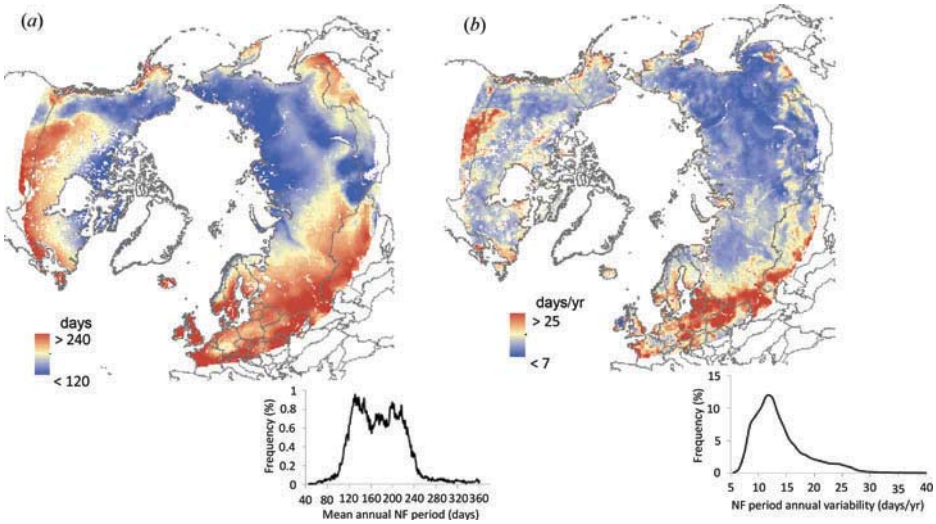

Figure 2. (*a*) The FT-ESDR-derived mean annual NF period (days) and (*b*) NF period annual variability (SD, days year^{-1}) derived from the 32 year (1979–2010) satellite (SMMR and SSM/I) microwave remote-sensing record; inset plots show the frequency distributions (% of total classified area) of the adjacent maps.

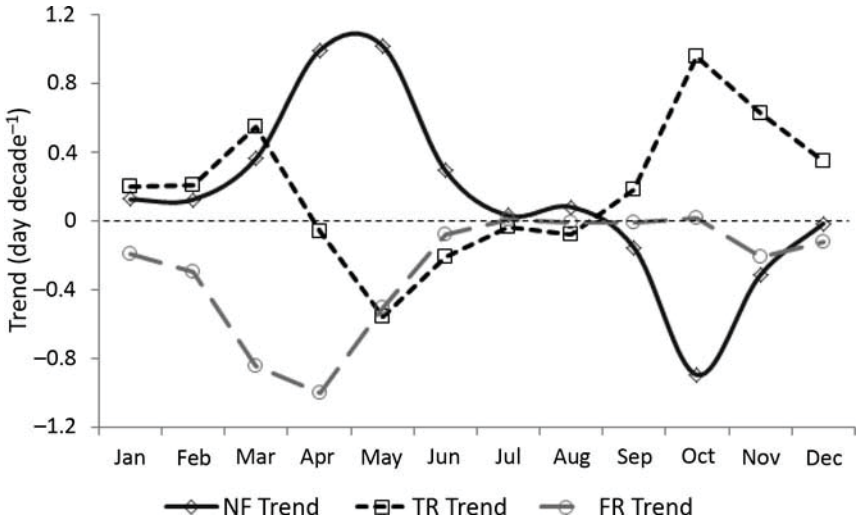

Figure 3. The HNL trends in regional monthly mean FT metrics for the 1979–2010 record, including the NF season, transitional (TR) frost days, and FR period.

spring is partially offset by a decreasing NF days' trend in the fall (SON), resulting in a smaller increasing annual NF season trend than might otherwise occur. A positive trend in the number of annual TR frost days (2.4 days decade^{-1}; $p < 0.1$) results from a strong TR increase from October to November. A significant decrease in the mean annual FR season (−3.0 days decade^{-1}; $p < 0.001$) is largely driven by a decreasing FR trend from March to May. An increase in the spring NF season is consistent with previous reports documenting warming trends in Arctic spring temperatures derived from model reanalysis (Screen, Deser, and Simmonds 2012). In fall, the decreasing NF days' trend coincides with a positive trend in the number of TR days, implying that the fall TR season is beginning earlier and extending over a longer period. The seasonal decrease in NF days and the corresponding increase in TR days imply regional cooling in the fall; the mechanisms for this apparent HNL cooling are uncertain but are consistent with reported increases in HNL moisture and snow cover in fall attributed to summer warming and sea ice decline (Cohen et al. 2012a, 2012b; Park et al. 2013). The recent increase in fall snow cover may promote regional cooling due to an enhanced snow-albedo feedback (Déry and Brown 2007).

Mean annual trends of $NDVI_{JJA}$ and NF_{JaAu} over the HNL domain are summarized in Table 1. The mean annual $NDVI_{JJA}$ records show general increasing trends of 5.6%

Table 1. Kendall's tau trends for mean annual $NDVI_{JJA}$ and NF_{JaAu} (value decade^{-1}) for the HNL domain and associated continental regions over the 1982–2010 NDVI record.

Trend	HNL (>45ºN)	NA	Eurasia
$NDVI_{JJA}$ [unit decade^{-1}]	0.023^{***}	0.02^{***}	0.025^{***}
(% decade^{-1})	(**5.61**)	(**5.67**)	(**5.64**)
NF_{JaAu} [days decade^{-1}]	3.319^{***}	3.052^{***}	3.43^{***}
(% decade^{-1})	(**3.59**)	(**7.47**)	(**2.69**)

Notes: Proportional changes (percent decade^{-1}) are denoted in bold, whereas trend significance levels are denoted by asterisks as: $^{*}p < 0.1$; $^{**}p < 0.01$; $^{***}p < 0.001$. Percent change is computed per year as 100 × (new value – original value)/(original value) and averaged for the 1982–2010 record.

decade^{-1} ($p < 0.001$) over the HNL domain from 1982 to 2010. The North American (NA) portion of the domain shows a mean $NDVI_{JJA}$ increase of 5.7% decade^{-1} ($p < 0.001$); Eurasia shows a similar mean $NDVI_{JJA}$ increase of 5.6% decade^{-1} ($p < 0.001$). The temporal trend in NF_{JaAu} is increasing at a rate of 3.6% decade^{-1} ($p < 0.001$) over the HNL domain. The FT-ESDR results also show positive NF_{JaAu} trends for NA and Eurasia of 7.5% decade^{-1} ($p < 0.001$) and 2.7% decade^{-1} ($p < 0.001$), respectively. These results indicate approximately 0.1% increase in NDVI summer growth for each day of increase in the HNL NF_{JaAu} season and 1982–2010 record.

3.3. NF season effects on vegetation canopy growth

The regional pattern (Figure 4) of correlations between the $NDVI_{JJA}$ and NF_{JaAu} anomalies shows generally positive correspondence above approximately 50º N (Figure 4(*c*)). There is a large drop in mean correlation at the highest latitudes due to the relatively lower quality (QA) of the FT classification and the smaller number of high-quality NDVI retrievals. Widespread negative correlations occur at lower latitudes over the HNL domain with a more heterogeneous pattern of positive and negative correlation areas. Areal proportions of positive and negative correlations between NF_{JaAu} and $NDVI_{JJA}$ anomalies are summarized for the four HNL biomes in Table 2. For the 29 year (1982–2010) NDVI record, tundra and boreal biomes show greater regional proportions of positive correspondence between NF_{JaAu} and $NDVI_{JJA}$ anomalies, whereas grassland and temperate forest biomes show similar areal proportions of positive and negative correlations. The NF_{JaAu} and $NDVI_{JJA}$ anomalies show widespread positive correlations over 68.1% of the HNL domain, including NA (70.4%) and Eurasian (64.2%) portions of the domain. Positive correspondence indicates that years with a longer NF_{JaAu} season relative to the long-term record coincide with greater summer vegetation canopy growth, whereas a negative correlation indicates that longer NF_{JaAu} seasons promote less vegetation growth. The correlation analysis indicates that NF_{JaAu} variability corresponds positively with $NDVI_{JJA}$ growth anomalies for a majority (>80%) of HNL boreal and tundra biomes, whereas correspondence is reduced or reversed for other areas.

3.4. Vegetation growth patterns within moisture- and temperature-constrained areas

The geographic distribution of estimated temperature (TSI) and moisture (MSI) control factors influencing vegetation activity over the HNL domain is presented in Figure 5. Dominant moisture-constraint cells are defined by positive difference ($Diff_{MSI–TSI} > 0$) values, whereas negative differences indicate cells with dominant temperature constraint ($Diff_{MSI–TSI} < 0$). The regional differences between MSI_{JJA} and TSI_{JJA} metrics averaged for the 1982–2010 period indicate that cold temperature constraints most strongly influence vegetation activity over 66.1% of the HNL domain and primarily within boreal and tundra biomes, whereas the temperature constraint to vegetation productivity is generally weaker in grassland and temperate forest regions, especially where plant-available moisture supply indicated by the MSI_{JJA} is a greater limitation to annual productivity (Figure 5). Areal proportions of dominant temperature-constrained areas over NA and Eurasia are 77.6% and 61.1%, respectively. Dominant temperature-constrained areas also occur along coastal margins, due to relatively more cloudiness and cooler growing seasons than other HNL areas. Dominant moisture-constrained areas are generally located in southern and inland continental regions of the HNL domain. These results are consistent with HNL continental interior areas showing vegetation browning associated with recent drought stress (Bi et al. 2013; Buermann et al. 2013; Goetz et al. 2005; Zhang et al. 2008).

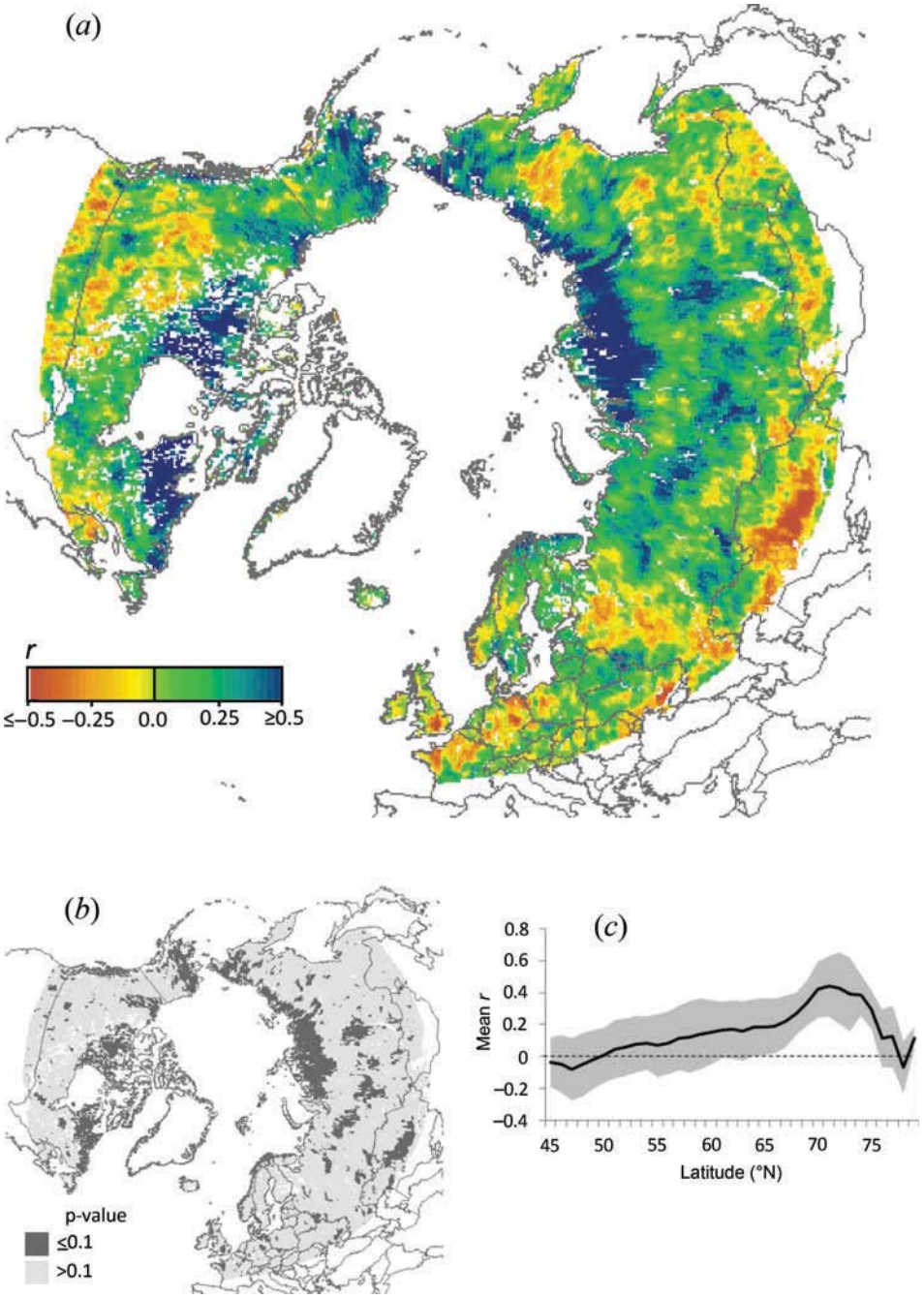

Figure 4. (*a*) Regional patterns of grid-cell-wise linear correlation coefficients (r) between $NDVI_{JJA}$ and NF_{JaAu} anomalies for the 1982–2010 NDVI record and HNL domain, (*b*) associated significance (*p*-value) map, and (*c*) mean *r*-values from the correlation map binned by latitude. Relatively lower quality FT classification results and smaller number of high-quality NDVI retrievals lead to a large drop in mean correlations at the highest latitudes. Error bars (grey shading) in (*c*) denote one SD range around the correlation means.

Table 2. Spatial extent of positive and negative correlations between NF_{JaAu} and $NDVI_{JJA}$ anomalies expressed as a proportion (%) of the regional biomes and the larger HNL domain; Four *r*-value categories are classified by significance level, including significant positive ($p \leq 0.1$), positive ($p > 0.1$), negative ($p > 0.1$), and significant negative ($p \leq 0.1$) levels.

	Sig. positive (%)	Positive (%)	Negative (%)	Sig. negative (%)
Tundra	45.8	45.3	8.8	0.1
Boreal Forests	19.2	60.4	19.8	0.5
Grasslands	4.0	44.2	48.3	3.5
Temperate Forests	3.6	44.5	48.2	3.7
HNL domain	17.0	51.1	29.4	2.6

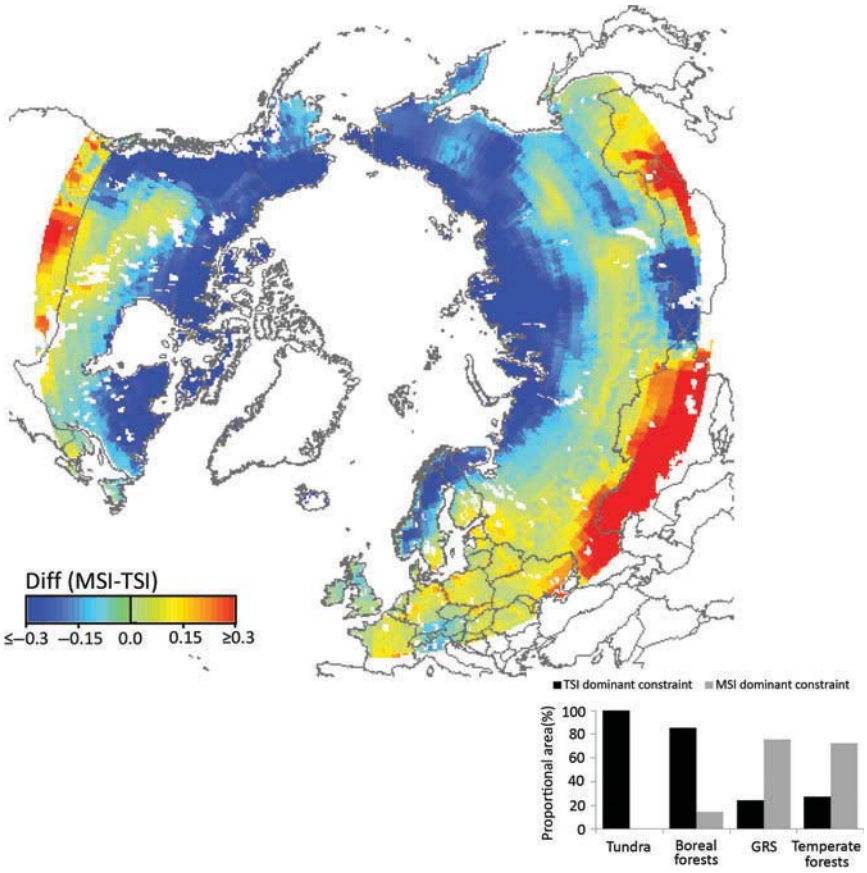

Figure 5. Geographic distribution of estimated summer vegetation moisture and temperature stress index differences over the HNL domain. Grid cells dominated by cold temperature (TSI) constraints are in blue, whereas cells dominated by summer moisture (MSI) constraints are in red. The proportions (%) of temperature- and moisture-constrained areas for individual biomes are shown in the inset map for tundra, boreal forests, grassland (GRS), and temperate forest areas.

The regional pattern of NF_{JaAu} and $NDVI_{JJA}$ correlations generally follows the pattern of estimated MSI and TSI dominance (Figure 6). A longer NF_{JaAu} season generally enhances $NDVI_{JJA}$ productivity in dominant cold temperature-constrained areas, while

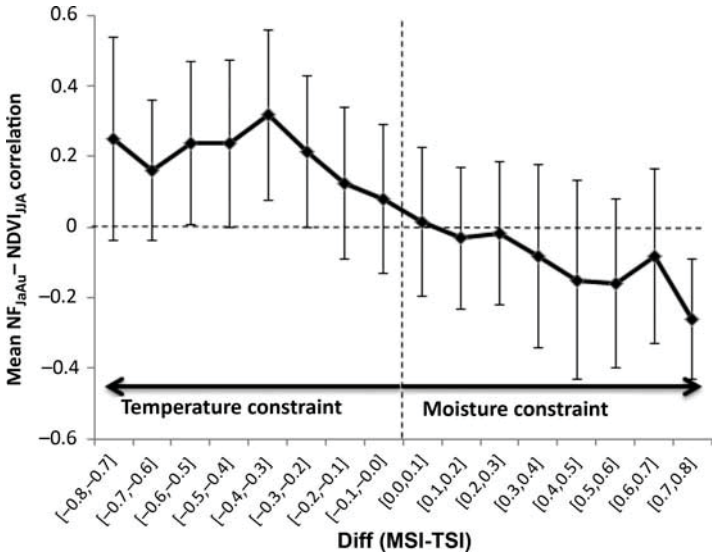

Figure 6. Mean correlation (r) of NF_{JaAu} and $NDVI_{JJA}$ relationships within the HNL domain relative to the strength of cold temperature (TSI)- and summer moisture (MSI)-constraint factors. Vertical bars denote the spatial SD of r-values.

the relative benefit of a longer NF season to vegetation growth is reduced or reversed in dominant moisture-constrained regions of the HNL domain. The sign of the NF_{JaAu} and $NDVI_{JJA}$ relationship is generally positive and negative for respective cold temperature- and moisture-dominant areas, whereas NF_{JaAu} and $NDVI_{JJA}$ correlation strength is proportional to the magnitude of TSI or MSI dominance. The relative strengths and regional patterns of the estimated temperature and moisture control factors may include substantial uncertainty associated with the coarse NNR surface meteorology used to derive the metrics (Buizza et al. 2005; Ma et al. 2008).

3.5. *FT impacts on atmospheric CO_2 seasonal cycle*

The HNL mean annual anomalies in FT-ESDR-defined T_{thaw} corresponded significantly ($p < 0.1$) with C_{spr} defined from GLOBALVIEW-CO_2 station observations over the 1979–2010 record (Figure 7). Temporal T_{thaw} and C_{spr} correspondence is predominantly positive ($r = 0.409$), indicating that relatively earlier (later) onset of the NF season coincides with earlier (later) growing season and C_{spr} drawdown. The HNL T_{thaw} anomaly for 1987 is approximately three-fold larger than other years of record and coincides with an extended period of TR frost days leading to a T_{thaw} delay for this year. The T_{thaw} anomaly also coincides with greater FT classification uncertainty and a lower annual FT-ESDR QA ranking for this year; the lower quality level was attributed to an extended gap in the satellite microwave T_b record following the inauguration of the SSM/I record in 1987 (Kim et al. 2012). A relatively early C_{spr} anomaly in 1990 is attributed to a shorter FR period in February and March relative to other years, and prior to the T_{thaw} event, whereas an anomalous C_{spr} delay for 1996 coincides with a longer FR period from January to April for this year. However, excluding outliers (1987, 1990, and 1996) from the correlation analysis resulted in similar T_{thaw} and C_{spr} correspondence ($r = 0.407$; $p < 0.1$).

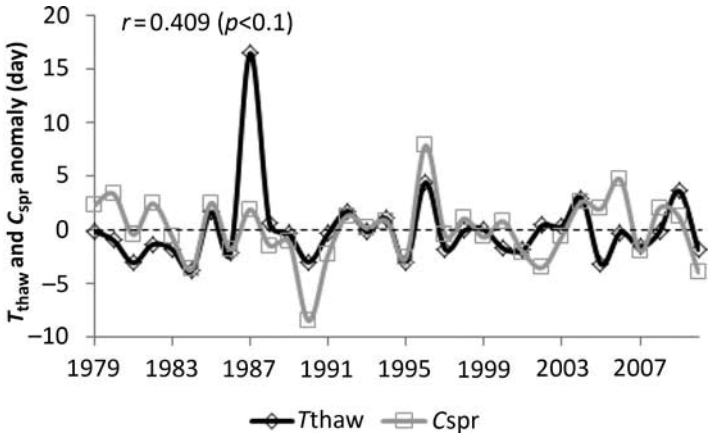

Figure 7. Temporal correlation between mean spring drawdown of northern atmospheric CO_2 (C_{spr}) concentrations from the GLOBALVIEW CO_2 record and FT-ESDR-derived annual mean primary spring thaw timing (T_{thaw}) for the HNL domain.

Correlations between HNL mean annual NF season variability and atmospheric CO_2 shape metrics anomalies for the 1979–2010 record were also analysed. We also examined these relationships over the shorter (1982–2010) record represented by the VIP NDVI record and found no difference in these relationships. Although the regional correlation between annual mean NF_{JaAu} and $NDVI_{JJA}$ anomalies indicates a general direct benefit of longer NF seasons to vegetation productivity ($r = 0.436$, $p < 0.05$ without outliers; not shown), the spatial correlation pattern (Figure 4) implies that the relative benefit of a longer NF period to productivity and net ecosystem CO_2 uptake is spatially variable, leading to a weak HNL mean NF_{JaAu} and C_{min} relationship ($r = –0.078$, $p > 0.1$; not shown). A positive correlation between HNL mean annual NF season and C_{end} anomalies ($r = 0.708$; $p < 0.001$) also accounts for the weak HNL NF and C_{min} relationship because longer (shorter) HNL NF seasons promote elevated (lower) seasonal CO_2 maximums for the region. These results imply that longer NF seasons enhance both photosynthetic carbon (CO_2) uptake and terrestrial carbon emissions, resulting in a net annual increase in atmospheric CO_2, whereas shorter NF seasons promote the opposite response. Potential sources of terrestrial carbon emissions associated with this response include soil heterotrophic respiration and disturbance, including wildfire and insect-related sources (Kurz et al. 2008; Randerson et al. 2006; Yi et al. 2013) and greater tree mortality (Hicke et al. 2012; Peng et al. 2011). However, the atmospheric CO_2 shape metrics may contain substantial uncertainty associated with strong annual CO_2 increase from fossil fuel emissions (Giorgi 2008).

4. Discussion and conclusions

The 1979–2010 FT-ESDR results show increasing HNL trends in the mean annual NF period (2.4 days decade^{-1}; $p < 0.005$) and NF_{JaAu} season (3.5 days decade^{-1}; $p < 0.001$) that are approximately 26% larger than the corresponding mean NF season trends for the larger Northern Hemisphere domain (Kim et al. 2012). An increasing NF_{JaAu} season trend occurs over 89% of the HNL domain, with 53% of the domain showing significant change relative to characteristic large annual NF season variability. These results

generally coincide with the areal proportion of decreasing snow-cover duration estimated from Northern Hemisphere meteorological stations for the 1980–2006 record (Peng et al. 2013). Our results indicate that each day of increase in the NF_{JaAu} season produces a relatively strong $NDVI_{JJA}$ increase (0.15 ± 0.2%) in dominant cold temperature-constrained areas, whereas the same NF increase produces a much smaller and insignificant growth increase (0.06 ± 0.1%) in dominant moisture-constrained HNL areas. A given daily increase in the NF season also produces a larger $NDVI_{JJA}$ increase in tundra (0.25 ± 0.2%) and boreal biomes (0.13 ± 0.2%), and relatively weak growth response in grassland (0.05 ± 0.1%) and temperate forest areas (0.06 ± 0.2%). Our FT and CO_2 correlation results confirm previous reports documenting a strong link between the timing of the primary spring thaw event defined from satellite microwave remote sensing and the onset of the vegetation growing season in northern biomes (Goetz et al. 2007; Kimball et al. 2004; McDonald et al. 2004). Our findings also support previous findings that a lengthening NF season coupled with increasing disturbance is likely to promote respiration and carbon emissions over productivity, diminishing HNL carbon sink strength (Angert et al. 2005; Yi et al. 2013).

The present geographic distribution of dominant moisture- and temperature-constrained regions indicates that a lengthening NF season is enhancing vegetation growth and productivity for a majority (82.8%) of HNL tundra and boreal biomes. These results are consistent with previous studies documenting satellite-derived HNL greening trends (Bhatt et al. 2010; Goetz et al. 2005; Xu et al. 2013). However, a longer NF season promotes reduced vegetation productivity benefits or adverse growth conditions for 51.9% of HNL grasslands and temperate forests due to summer water supply (MSI) restrictions to plant growth. Strengthening evaporative demands and more frequent summer droughts associated with earlier snowmelt and warmer summer temperatures may lead to more severe negative impacts on vegetation growth in more moisture-constrained areas (Barnett, Adam, and Lettenmaier 2005; Jepsen et al. 2012). These results are similar to previous studies indicating widespread drought-induced vegetation productivity declines in northern temperate and boreal forests (Beck and Goetz 2011; Piao et al. 2011; Ma et al. 2012).

The positive correspondence between HNL mean T_{thaw} and C_{spr} anomalies indicates that earlier spring thawing promotes generally earlier ecosystem carbon (CO_2) uptake. Abundant spring solar radiation coupled with earlier seasonal thawing promotes deeper soil active layer development and release of plant-available moisture and nutrients, leading to rapid vegetation carbon uptake and earlier C_{spr} (Bergh and Linder 1999; Tanja et al. 2003; Wang et al. 2011). However, our results indicate that longer NF seasons also promote increased amplitude of the atmospheric CO_2 seasonal cycle; thus the relative increase in CO_2 uptake by ecosystem productivity is being offset by enhanced carbon emissions, likely due to commensurate increases in regional disturbance and respiration processes (Angert et al. 2005; Buermann et al. 2013; Kasischke et al. 2005).

The results of this study document a consistent increase in the annual NF season over northern land areas from 1979 to 2010 as derived from the satellite passive microwave remote-sensing record. The lengthening NF season is consistent with global warming and appears to be largely benefitting HNL vegetation productivity, inferred from satellite NDVI summer growth changes, by promoting earlier and longer growing seasons. However, the relative benefits for vegetation productivity do not appear to be increasing terrestrial carbon sink activity indicated from the regional atmospheric CO_2 record, as carbon emissions from enhanced disturbance and respiration processes appear to be offsetting CO_2 uptake from additional vegetation growth. Our results also indicate that

the relative benefits of a lengthening NF season for vegetation growth are spatially heterogeneous and are reduced or reversed in dominant moisture (MSI)-constrained areas, including grassland and northern temperate forest areas. A lengthening NF season is expected to continue to benefit productivity in dominant cold temperature (TSI)-constrained regions, including tundra, although these constraints will likely relax with associated contraction of dominant TSI-constrained areas under continued HNL warming. In contrast, dominant moisture (MSI)-constrained areas are expected to become more widespread, with more persistent and severe summer drought constraints (Goetz et al. 2005; Ma et al. 2012). These changes are likely to promote a net decrease in HNL vegetation productivity and the terrestrial carbon sink without commensurate increases in regional precipitation and terrestrial water storage required to offset expected increases in evaporative demands under a warming climate (Hayes et al. 2011; Parmentier et al. 2011; Schuur et al. 2008).

Funding

This work was conducted at the University of Montana under contract to the National Aeronautics and Space Administration, with funding support provided by the NASA Terrestrial Ecology and Hydrology programmes. The FT-ESDR and VIP NDVI data records used for this investigation were provided by the National Snow and Ice Data Center (NSIDC) and the University of Arizona, with funding support provided by the NASA measures (*Making Earth System Data Records for Use in Research Environments*) programme. The GLOBALVIEW-CO_2 data record used for this study was provided by the NOAA ESRL (*Earth System Research Laboratory*).

References

Akritas, M. G., S. A. Murphy, and M. P. LaValley. 1995. "The Theil-Sen Estimator with Doubly Censored Data and Applications to Astronomy." *Journal of the American Statistical Association* 90 (429): 170–177. doi:10.1080/01621459.1995.10476499.

Alcaraz-Segura, D., E. Chuvieco, H. E. Epstein, E. S. Kasischke, and A. Trishchenko. 2010. "Debating the Greening Vs. Browning of the North American Boreal Forest: Differences between Satellite Datasets." *Global Change Biology* 16: 760–770. doi:10.1111/j.1365–2486.2009.01956.x.

Alvera-Azcárate, A., D. Sirjacobs, A. Barth, and J. M. Beckers. 2012. "Outlier Detection in Satellite Data Using Spatial Coherence." *Remote Sensing of Environment* 119: 84–91. doi:10.1016/j.rse.2011.12.009.

Angert, A., S. Biraud, C. Bonfils, C. C. Henning, W. Buermann, J. Pinzon, C. J. Tucker, and I. Fung. 2005. "Drier Summers Cancel Out the CO_2 Uptake Enhancement Induced by Warmer Springs." *Proceedings of the National Academy of Sciences of the United States of America* 102 (31): 10823–10827. doi:10.1073/pnas.0501647102.

Baird, R. A., D. Verbyla, and T. N. Hollingsworth. 2012. "Browning of the Landscape of Interior Alaska Based on 1986–2009 Landsat Sensor NDVI." *Canadian Journal of Forest Research* 42: 1371–1382. doi:10.1139/x2012-088.

Barnett, T. P., J. C. Adam, and D. P. Lettenmaier. 2005. "Potential Impacts of a Warming Climate on Water Availability in Snow-Dominated Regions." *Nature* 438: 303–309. doi:10.1038/nature04141.

Beck, P. S. A., and S. J. Goetz. 2011. "Satellite Observations of High Northern Latitude Vegetation Productivity Changes between 1982 and 2008: Ecological Variability and Regional Differences." *Environmental Research Letters* 6: 049501. doi:10.1088/1748-3182/6/4/049501.

Beck, P. S. A., G. P. Juday, C. Alix, V. A. Barber, S. E. Winslow, E. E. Sousa, P. Heiser, J. D. Herriges, and S. J. Goetz. 2011. "Changes in Forest Productivity across Alaska Consistent with Biome Shift." *Ecology Letters* 14 (4): 373–379. doi:10.1111/j.1461-0248.2011.01598.x.

Bergh, J., and S. Linder. 1999. "Effects of Soil Warming during Spring on Photosynthetic Recovery in Boreal Norway Spruce Stands." *Global Change Biology* 5: 245–253. doi:10.1046/j.1365-2486.1999.00205.x.

Bhatt, U. S., D. A. Walker, M. K. Raynolds, J. C. Comiso, H. E. Epstein, G. Jia, R. Gens, J. E. Pinzon, C. J. Tucker, C. E. Tweedie, and P. J. Webber. 2010. "Circumpolar Arctic Tundra Vegetation Change is Linked to Sea Ice Decline." *Earth Interactions* 14 (8): 1–20. doi:10.1175/2010EI315.1.

Bi, J., L. Xu, A. Samanta, Z. Zhu, and R. Myneni. 2013. "Divergent Arctic-Boreal Vegetation Changes between North America and Eurasia over the past 30 Years." *Remote Sensing* 5: 2093–2112. doi:10.3390/rs5052093.

Bond-Lamberty, B., S. D. Peckham, D. E. Ahl, and S. T. Gower. 2007. "Fire as the Dominant Driver of Central Canadian Boreal Forest Carbon Balance." *Nature* 450: 89–92. doi:10.1038/nature06272.

Brodzik, M. J., and K. W. Knowles. 2002. "Ease-Grid: A Versatile Set of Equal-Area Projections and Grids." In *Discrete Global Grids*, edited by M. Goodchild. Santa Barbara, CA: National Center for Geographic Information and Analysis.

Buermann, W., P. R. Bikash, M. Jung, D. H. Burn, and M. Reichstein. 2013. "Earlier Springs Decrease Peak Summer Productivity in North American Boreal Forests." *Environmental Research Letters* 8 (2): 024027. doi:10.1088/1748–9326/8/2/024027.

Buizza, R., P. L. Houtekamer, G. Pellerin, Z. Toth, Y. Zhu, and M. Wei. 2005. "A Comparison of the ECMWF, MSC, and NCEP Global Ensemble Prediction Systems." *Monthly Weather Review* 133: 1076–1097. doi:10.1175/MWR2905.1.

Bunn, A. G., and S. J. Goetz. 2006. "Trends in Satellite-Observed Circumpolar Photosynthetic Activity from 1982 to 2003: The Influence of Seasonality, Cover Type, and Vegetation Density." *Earth Interactions* 10 (12): 1–19. doi:10.1175/EI190.1.

Cohen, J. L., J. C. Furtado, M. Barlow, V. A. Alexeev, and J. E. Cherry. 2012b. "Asymmetric Seasonal Temperature Trends." *Geophysical Research Letters* 39: L04705. doi:10.1029/2011GL050582.

Cohen, J. L., J. C. Furtado, M. A. Barlow, V. A. Alexeev, and J. E. Cherry. 2012a. "Arctic Warming, Increasing Snow Cover and Widespread Boreal Winter Cooling." *Environmental Research Letters* 7: 014007. doi:10.1088/1748–9326/7/1/014007.

de Beurs, K. M., and G. M. Henebry. 2005. "A Statistical Framework for the Analysis of Long Image Time Series." *International Journal of Remote Sensing* 26 (8): 1551–1573. doi:10.1080/01431160512331326657.

de Jong, R., S. de Bruin, A. de Wit, M. E. Schaepman, and D. L. Dent. 2011. "Analysis of Monotonic Greening and Browning Trends from Global NDVI Time-Series." *Remote Sensing of Environment* 115: 692–702. doi:10.1016/j.rse.2010.10.011.

Déry, S. J., and R. D. Brown. 2007. "Recent Northern Hemisphere Snow Cover Extent Trends and Implications for the Snow-Albedo Feedback." *Geophysical Research Letters* 34: L22504. doi:10.1029/2007GL031474.

Didan, K. 2010. "Multi-Satellite Earth Science Data Record for Studying Global Vegetation Trends and Changes." IGARSS2010.

Drobot, S., J. Maslanik, U. C. Herzfeld, C. Fowler, and W. Wu. 2006. "Uncertainty in Temperature and Precipitation Datasets over Terrestrial Regions of the Western Arctic." *Earth Interactions* 10 (23): 1–17. doi:10.1175/EI191.1.

Dye, D. G., and C. J. Tucker. 2003. "Seasonality and Trends of Snow-Cover, Vegetation Index, and Temperature in Northern Eurasia." *Geophysical Research Letters* 30 (7): 1405. doi:10.1029/2002GL016384.

Field, C. B., J. T. Randerson, and C. M. Malmström. 1995. "Global Net Primary Production: Combining Ecology and Remote Sensing." *Remote Sensing of Environment* 51: 74–88. doi:10.1016/0034-4257(94)00066-V.

Friedlingstein, P., P. Cox, R. Betts, L. Bopp, W. von Bloh, V. Brovkin, P. Cadule, S. Doney, M. Eby, I. Fung, G. Bala, J. John, C. Jones, F. Joos, T. Kato, M. Kawamiya, W. Knorr, K. Lindsay, H. D. Matthews, T. Raddatz, P. Rayner, C. Reick, E. Roeckner, K. Schnitzler, R. Schnur, K. Strassmann, A. J. Weaver, C. Yoshikawa, and N. Zeng. 2006. "Climate-Carbon Cycle Feedback Analysis: Results from the C4MIP Model Intercomparison." *Journal of Climate* 19: 3337–3353. doi:10.1175/JCLI3800.1.

Giorgi, F. 2008. "A Simple Equation for Regional Climate Change and Associated Uncertainty." *Journal of Climate* 21: 1589–1604. doi:10.1175/2007JCLI1763.1.

Girardin, M. P., and M. Mudelsee. 2008. "Past and Future Changes in Canadian Boreal Wildfire Activity." *Ecological Applications* 18 (2): 391–406. doi:10.1890/07–0747.1.

GLOBALVIEW-CO_2. 2011. C*ooperative Atmospheric Data Integration Project – Carbon Dioxide*. CD-ROM, NOAA ESRL, Boulder, CO. Accessed June 3, 2013. [Also available on internet via anonymous FTP to ftp.cmdl.noaa.gov, Path: ccg/co_2/GLOBALVIEW.]

Goetz, S. J., B. Bond-Lamberty, B. E. Law, J. A. Hicke, C. Huang, R. A. Houghton, S. McNulty, T. O'Halloran, M. Harmon, A. J. H. Meddens, E. M. Pfeifer, D. Mildrexler, and E. S. Kasischke. 2012. "Observations and Assessment of Forest Carbon Dynamics Following Disturbance in North America." *Journal of Geophysical Research: Biogeosciences* 117: G02022. doi:10.1029/2011JG001733.

Goetz, S. J., A. G. Bunn, G. J. Fiske, and R. A. Houghton. 2005. "Satellite-Observed Photosynthetic Trends across Boreal North America Associated with Climate and Fire Disturbance." *Proceedings of the National Academy of Sciences of the United States of America* 102 (38): 13521–13525. doi:10.1073/pnas.0506179102.

Goetz, S. J., M. C. Mack, K. R. Gurney, J. T. Randerson, and R. A. Houghton. 2007. "Ecosystem Responses to Recent Climate Change and Fire Disturbance at Northern High Latitudes: Observations and Model Results Contrasting Northern Eurasia and North America." *Environmental Research Letters* 2: 045031. doi:10.1088/1748-9326/2/4/045031.

Hall, F., J. G. Masek, and G. J. Collatz. 2006. "Evaluation of ISLSCP Initiative II FASIR and GIMMS NDVI Products and Implications for Carbon Cycle Science." *Journal of Geophysical Research* 111: D22S08. doi:10.1029/2006JD007438.

Hayes, D. J., A. D. McGuire, D. W. Kicklighter, K. R. Gurney, T. J. Burnside, and J. M. Melillo. 2011. "Is the Northern High-Latitude Land-Based CO_2 Sink Weakening?" *Global Biogeochemical Cycles* 25: GB3018. doi:10.1029/2010GB003813.

Hicke, J. A., C. D. Allen, A. R. Desai, M. C. Dietze, R. J. Hall, E. H. Hogg, D. M. Kashian, D. Moore, K. F. Raffa, R. N. Sturrock, and J. Vogelmann. 2012. "Effects of Biotic Disturbances on Forest Carbon Cycling in the United States and Canada." *Global Change Biology* 18: 7–34. doi:10.1111/j.1365-2486.2011.02543.x.

Higuchi, K., D. Worthy, D. Chan, and A. Shashkov. 2003. "Regional Source/Sink Impact on the Diurnal, Seasonal and Inter-Annual Variations in Atmospheric CO_2 at A Boreal Forest Site in Canada." *Tellus B* 55: 115–125. doi:10.1034/j.1600-0889.2003.00062.x.

Hudson, J. M., and H. R. Henry. 2009. "Increased Plant Biomass in a High Arctic Heath Community from 1981 to 2008." *Ecology* 90 (10): 2657–2663. doi:10.1890/09-0102.1.

Huete, A. R., K. Didan, T. Miura, E. P. Rodriguez, X. Gao, and L. G. Ferreira. 2002. "Overview of the Radiometric and Biophysical Performance of the MODIS Vegetation Indices." *Remote Sensing of Environment* 83: 195–213. doi:10.1016/S0034-4257(02)00096-2.

Jepsen, S. M., N. P. Molotch, M. W. Williams, K. E. Rittger, and J. O. Sickman. 2012. "Interannual Variability of Snowmelt in the Sierra Nevada and Rocky Mountains, United States: Examples from Two Alpine Watersheds." *Water Resources Research* 48: W02529. doi:10.1029/2011WR011006.

Jones, L. A., C. R. Ferguson, J. S. Kimball, K. Zhang, S. T. K. Chan, K. C. McDonald, E. G. Njoku, and E. F. Wood. 2010. "Satellite Microwave Remote Sensing of Daily Land Surface Air Temperature Minima and Maxima from AMSR-E." *IEEE Journal of Selected Topics in Applied Earth Observations and Remote Sensing* 3 (1): 111–123. doi:10.1109/JSTARS.2010.2041530.

Kalnay, E., M. Kanamitsu, R. Kistler, W. Collins, D. Deaven, L. Gandin, M. Iredell, S. Saha, G. White, J. Woollen, Y. Zhu, M. Chelliah, W. Ebisuzaki, W. Higgins, J. Janowiak, K. C. Mo, C. Ropelewski, J. Wang, A. Leetmaa, R. Reynolds, R. Jenne, and D. Joseph. 1996. "The NCEP/NCAR 40-Year Reanalysis Project." *Bulletin of the American Meteorological Society* 77: 437–471. doi:10.1175/1520-0477(1996)077<0437:TNYRP>2.0.CO;2.

Kanamitsu, M., W. Ebisuzaki, J. Woollen, S. Yang, J. J. Hnilo, M. Fiorino, and G. L. Potter. 2002. "NCEP-DOE AMIP-II Reanalysis (R-2)." *Bulletin of the American Meteorological Society* 83: 1631–1643. doi:10.1175/BAMS-83-11-1631.

Kasischke, E. S., E. J. Hyer, P. C. Novelli, L. P. Bruhwiler, N. H. F. French, A. I. Sukhinin, J. H. Hewson, and B. J. Stocks. 2005. "Influences of Boreal Fire Emissions on Northern Hemisphere Atmospheric Carbon and Carbon Monoxide." *Global Biogeochemical Cycles* 19: GB1012. doi:10.1029/2004GB002300.

Kim, Y., J. S. Kimball, J. Glassy, and K. McDonald 2013. *Measures Global Record of Daily Landscape Freeze/Thaw Status, Version 2, [1979 to 2010]*. Boulder, CO: National Snow and Ice Data Center. Digital media. Accessed June 3, 2013. http://nsidc.org/data/nsidc-0477.html

Kim, Y., J. S. Kimball, K. C. McDonald, and J. Glassy. 2011. "Developing a Global Data Record of Daily Landscape Freeze/Thaw Status Using Satellite Passive Microwave Remote Sensing." *IEEE Transactions on Geoscience and Remote Sensing* 49 (3): 949–960. doi:10.1109/TGRS.2010.2070515.

Kim, Y., J. S. Kimball, K. Zhang, and K. C. McDonald. 2012. "Satellite Detection of Increasing Northern Hemisphere Non-Frozen Seasons from 1979 to 2008: Implications for Regional Vegetation Growth." *Remote Sensing of Environment* 121: 472–487. doi:10.1016/j.rse.2012.02.014.

Kimball, J. S., K. C. McDonald, S. W. Running, and S. E. Frolking. 2004. "Satellite Radar Remote Sensing of Seasonal Growing Seasons for Boreal and Subalpine Evergreen Forests." *Remote Sensing of Environment* 90: 243–258. doi:10.1016/j.rse.2004.01.002.

Kimball, J. S., K. C. McDonald, and M. Zhao. 2006. "Spring Thaw and its Effect on Terrestrial Vegetation Productivity in the Western Arctic Observed from Satellite Microwave and Optical Remote Sensing." *Earth Interactions* 10 (21): 1–22. doi:10.1175/EI187.1.

Kimball, J. S., M. Zhao, A. D. McGuire, F. A. Heinsch, J. Clein, M. Calef, W. M. Jolly, S. Kang, S. E. Euskirchen, K. C. McDonald, and S. W. Running. 2007. "Recent Climate-Driven Increases in Vegetation Productivity for the Western Arctic: Evidence of an Acceleration of the Northern Terrestrial Carbon Cycle." *Earth Interactions* 11 (4): 1–30. doi:10.1175/EI180.1.

Kistler, R., E. Kalnay, W. Collins, S. Saha, G. White, J. Woollen, M. Chelliah, W. Ebisuzaki, M. Kanamitsu, V. Kousky, H. Dool, R. Jenne, and M. Fiorino. 2001. "The NCEP-NCAR 50-year Reanalysis: Monthly Means CD-ROM and Documentation." *Bulletin of the American Meteorological Society* 82: 247–268. doi:10.1175/1520-0477(1996)077<0437:TNYRP>2.0.CO;2.

Kurz, W. A., C. C. Dymond, G. Stinson, G. J. Rampley, E. T. Neilson, A. L. Carroll, T. Ebata, and L. Safranyik. 2008. "Mountain Pine Beetle and Forest Carbon Feedback to Climate Change." *Nature* 452: 987–990. doi:10.1038/nature06777.

Le Quéré, C., M. R. Raupach, J. G. Canadell, G. Marland, L. Bopp, P. Ciais, T. J. Conway, S. C. Doney, R. A. Feely, P. Foster, P. Friedlingstein, K. Gurney, R. A. Houghton, J. I. House, C. Huntingford, P. E. Levy, M. R. Lomas, J. Majkut, N. Metzl, J. P. Ometto, G. P. Peters, I. C. Prentice, J. T. Randerson, S. W. Running, J. L. Sarmiento, U. Schuster, S. Sitch, T. Takahashi, N. Viovy, G. R. van der Werf, and F. I. Woodward. 2009. "Trends in the Sources and Sinks of Carbon Dioxide." *Nature Geoscience* 2: 831–836. doi:10.1038/ngeo689.

Liu, J., J. A. Curry, Y. Dai, and R. Horton. 2007. "Causes of the Northern High-Latitude Land Surface Winter Climate Change." *Geophysical Research Letters* 34: L14702. doi:10.1029/2007GL030196.

Lloyd, A. H., A. G. Bunn, and L. Berner. 2011. "A Latitudinal Gradient in Tree Growth Response to Climate Warming in the Siberian Taiga." *Global Change Biology* 17: 1935–1945. doi:10.1111/j.1365-2486.2010.02360.x.

Lucht, W. S., S. T. Schaphoff, T. Erbrecht, U. Heyder, and W. Cramer. 2006. "Terrestrial Vegetation Redistribution and Carbon Balance under Climate Change." *Carbon Balance and Management* 1: 6–13. doi:10.1186/1750-0680-1-6.

Ma, L., T. Zhang, Q. Li, O. W. Frauenfeld, and D. Qin. 2008. "Evaluation of ERA-40, NCEP-1, and NCEP-2 Reanalysis Air Temperatures with Ground-Based Measurements in China." *Journal of Geophysical Research* 113: D15115. doi:10.1029/2007JD009549.

Ma, Z., C. Peng, Q. Zhu, H. Chen, G. Yu, W. Li, X. Zhou, W. Wang, and W. Zhang. 2012. "Regional Drought-Induced Reduction in the Biomass Carbon Sink of Canada's Boreal Forests." *Proceedings of the National Academy of Sciences of the United States of America* 109: 2423–2427. doi:10.1073/pnas.1111576109.

Masarie, K. A., and P. P. Tans. 1995. "Extension and Integration of Atmospheric Carbon Dioxide Data into a Globally Consistent Measurement Record." *Journal of Geophysical Research* 100 (D6): 11593–11610. doi:10.1029/95JD00859.

McCloy, K. R., S. Los, W. Lucht, and S. Hojsgaard. 2005. "A Comparative Analysis of Three Long-Term NDVI Datasets Derived from AVHRR Satellite Data." *EARSel eProceedings* 4 (1): 52–69.

McDonald, K. C., J. S. Kimball, E. Njoku, R. Zimmermann, and M. Zhao. 2004. "Variability in Springtime Thaw in the Terrestrial High Latitudes: Monitoring a Major Control on the Biospheric Assimilation of Atmospheric CO_2 with Spaceborne Microwave Remote Sensing." *Earth Interactions* 8 (20): 1–23. doi:10.1175/1087-3562(2004)8<1:VISTIT>2.0.CO;2.

McGuire, A. D., L. G. Anderson, T. R. Christensen, S. Dallimore, L. Guo, D. J. Hayes, M. Heimann, T. D. Lorenson, R. W. MacDonald, and N. Roulet. 2009. "Sensitivity of the

Carbon Cycle in the Arctic to Climate Change." *Ecological Monographs* 79 (4): 523–555. doi:10.1890/08-2025.1.

McGuire, A. D., J. M. Melillo, D. W. Kicklighter, and L. A. Joyce. 1995. "Equilibrium Responses of Soil Carbon to Climate Change: Empirical and Process-Based Estimates." *Journal of Biogeography* 22: 785–796. doi:10.2307/2845980.

McManus, K. M., D. C. Morton, J. G. Masek, D. Wang, J. O. Sexton, J. R. Nagol, P. Ropars, and S. Boudreau. 2012. "Satellite-Based Evidence for Shrub and Graminoid Tundra Expansion in Northern Quebec from 1986 to 2010." *Global Change Biology* 18: 2313–2323. doi:10.1111/j.1365-2486.2012.02708.x.

Miura, T., A. Huete, and H. Yoshioka. 2006. "An Empirical Investigation of Cross-Sensor Relationships of NDVI and Red/Near-Infrared Reflectance Using EO-1 Hyperion Data." *Remote Sensing of Environment* 100: 223–236. doi:10.1016/j.rse.2005.10.010.

Moore, D. S. 2006. *Introduction to the Practice of Statistics*. 5th ed. New York, NY: W.H. Freeman and Company.

Murayama, S., S. Taguchi, and K. Higuchi. 2004. "Interannual Variation in the Atmospheric CO_2 Growth Rate: Role of Atmospheric Transport in the Northern Hemisphere." *Journal of Geophysical Research* 109: D02305. doi:10.1029/2003JD003729.

Naeimi, V., C. Paulik, A. Bartsch, W. Wagner, R. Kidd, S. Park, K. Elger, and J. Boike. 2012. "ASCAT Surface State Flag (SSF): Extracting Information on Surface Freeze/Thaw Conditions from Backscatter Data Using an Empirical Threshold-Analysis Algorithm." *IEEE Transactions on Geoscience and Remote Sensing* 50 (7): 2566–2582. doi:10.1109/TGRS.2011.2177667.

Nagol, J. R., E. F. Vermote, and S. D. Prince. 2009. "Effects of Atmospheric Variation on AVHRR NDVI Data." *Remote Sensing of Environment* 113: 392–397. doi:10.1016/j.rse.2008.10.007.

Nemani, R. R., C. D. Keeling, H. Hashimoto, W. M. Jolly, S. C. Piper, C. J. Tucker, R. B. Myneni, and S. W. Running. 2003. "Climate-Driven Increases in Global Terrestrial Net Primary Production from 1982 to 1999." *Science* 300: 1560–1563. doi:10.1126/science.1082750.

Olson, D. M., E. Dinerstein, E. D. Wikramanayake, N. D. Burgess, G. V. N. Powell, E. C. Underwood, J. A. D'Amico, I. Itoua, H. E. Strand, J. C. Morrison, C. J. Loucks, T. F. Allnutt, T. H. Ricketts, Y. Kura, J. F. Lamoreux, W. W. Wettengel, P. Hedao, and K. R. Kassem. 2001. "Terrestrial Ecoregions of the World: A New Map of Life on Earth." *Bioscience* 51 (11): 933–938. doi:10.1641/0006-3568(2001)051[0933:TEOTWA]2.0.CO;2.

Park, H., and B. J. Sohn. 2010. "Recent Trends in Changes of Vegetation over East Asia Coupled with Temperature and Rainfall Variations." *Journal of Geophysical Research* 115: D14101. doi:10.1029/2009JD012752.

Park, H., J. E. Walsh, Y. Kim, T. Nakai, and T. Ohata. 2013. "The Role of Declining Arctic Sea Ice in Recent Decreasing Terrestrial Arctic Snow Depths." *Polar Science* 7: 174–187. doi:10.1016/j.polar.2012.10.002.

Parmentier, F. J. W., M. K. van der Molen, J. van Huissteden, S. A. Karsanaev, A. V. Kononov, D. A. Suzdalov, T. C. Maximov, and A. J. Dolman. 2011. "Longer Growing Seasons Do Not Increase Net Carbon Uptake in the Northeastern Siberian Tundra." *Journal of Geophysical Research* 116: G04013. doi:10.1029/2011JG001653.

Patra, P. K., M. Ishizawa, S. Maksyutov, T. Nakazawa, and G. Inoue. 2005. "Role of Biomass Burning and Climate Anomalies for Land-Atmosphere Carbon Fluxes Based on Inverse Modeling of Atmospheric CO_2." *Global Biogeochemical Cycles* 19: GB3005. doi:10.1029/2004GB002258.

Peng, C., Z. Ma, X. Lei, Q. Zhu, H. Chen, W. Wang, S. Liu, W. Li, X. Fang, and X. Zhou. 2011. "A Drought-Induced Pervasive Increase in Tree Mortality across Canada's Boreal Forests." *Nature Climate Change* 1: 467–471. doi:10.1038/nclimate1293.

Peng, S., S. Piao, P. Ciais, P. Friedlingstein, L. Zhou, and T. Wang. 2013. "Change in Snow Phenology and Its Potential Feedback to Temperature in the Northern Hemisphere over the Last Three Decades." *Environmental Research Letters* 8: 014008. doi:10.1088/1748-9326/8/1/014008.

Piao, S., X. Wang, P. Ciais, B. Zhu, T. Wang, and J. Liu. 2011. "Changes in Satellite-Derived Vegetation Growth Trend in Temperate and Boreal Eurasia from 1982 to 2006." *Global Change Biology* 17: 3228–3239. doi:10.1111/j.1365-2486.2011.02419.x.

Pouliot, D., R. Latifovic, and I. Olthof. 2009. "Trends in Vegetation NDVI from 1 Km AVHRR Data over Canada for the Period 1985–2006." *International Journal of Remote Sensing* 30 (1): 149–168. doi:10.1080/01431160802302090.

Qian, H., R. Joseph, and N. Zeng. 2010. "Enhanced Terrestrial Carbon Uptake in the Northern High Latitudes in the 21st Century from the Coupled Carbon Cycle Climate Model Intercomparison Project Model Projections." *Global Change Biology* 16: 641–656. doi:10.1111/j.1365-2486.2009.01989.x.

Randerson, J. T., C. B. Field, I. Y. Fung, and P. P. Tans. 1999. "Increases in Early Season Ecosystem Uptake Explain Recent Changes in the Seasonal Cycle of Atmospheric CO_2 at High Northern Latitudes." *Geophysical Research Letters* 26 (17): 2765–2768. doi:10.1029/1999GL900500.

Randerson, J. T., H. Liu, M. G. Flanner, S. D. Chambers, Y. Jin, P. G. Hess, G. Pfister, M. C. Mack, K. K. Treseder, L. R. Welp, F. S. Chapin, J. W. Harden, M. L. Goulden, E. Lyons, J. C. Neff, E. A. G. Schuur, and C. S. Zender. 2006. "The Impact of Boreal Forest Fire on Climate Warming." *Science* 314: 1130–1132. doi:10.1126/science.1132075.

Randerson, J. T., M. V. Thompson, T. J. Conway, I. Y. Fung, and C. B. Field. 1997. "The Contribution of Terrestrial Sources and Sinks to Trends in the Seasonal Cycle of Atmospheric Carbon Dioxide." *Global Biogeochemical Cycles* 11 (4): 535–560. doi:10.1029/97GB02268.

Rawlins, M. A., S. Frolking, R. B. Lammers, and C. J. Vörösmarty. 2006. "Effects of Uncertainty in Climate Inputs on Simulated Evapotranspiration and Runoff in the Western Arctic." *Earth Interactions* 10 (18): 1–18. doi:10.1175/EI182.1.

Raynolds, M. K., D. A. Walker, H. E. Epstein, J. E. Pinzon, and C. J. Tucker. 2012. "A New Estimate of Tundra-Biome Phytomass from Trans-Arctic Field Data and AVHRR NDVI." *Remote Sensing Letters* 3 (5): 403–411. doi:10.1080/01431161.2011.609188.

Schaphoff, S., W. Lucht, D. Gerten, S. Sitch, W. Cramer, and I. C. Prentice. 2006. "Terrestrial Biosphere Carbon Storage under Alternative Climate Projections." *Climatic Change* 74: 97–122. doi:10.1007/s10584-005-9002-5.

Schuur, E. A. G., J. Bockheim, J. G. Canadell, E. Euskirchen, C. B. Field, S. V. Goryachkin, S. Hagemann, P. Kuhry, P. M. Lafleur, H. Lee, G. Mazhitova, F. E. Nelson, A. Rinke, V. E. Romanovsky, N. Shiklomanov, C. Tarnocai, S. Venevsky, J. G. Vogel, and S. A. Zimov. 2008. "Vulnerability of Permafrost Carbon to Climate Change: Implications for the Global Carbon Cycle." *Bioscience* 58 (8): 701–714. doi:10.1641/B580807.

Screen, J. A., C. Deser, and I. Simmonds. 2012. "Local and Remote Controls on Observed Arctic Warming." *Geophysical Research Letters* 39: L10709. doi:10.1029/2012GL051598.

Sen, P. K. 1968. "Estimates of the Regression Coefficient Based on Kendall's Tau." *Journal of the American Statistical Association* 63 (324): 1379–1389. doi:10.1080/01621459.1968.10480934.

Serreze, M. C., and J. A. Francis. 2006. "The Arctic Amplification Debate." *Climatic Change* 76: 241–264. doi:10.1007/s10584-005-9017-y.

Shuai, Y., C. B. Schaaf, A. H. Strahler, J. Liu, and Z. Jiao. 2008. "Quality Assessment of Brdf/Albedo Retrievals in MODIS Operational System." *Geophysical Research Letters* 35: L05407. doi:10.1029/2007GL032568.

Simmons, A. J., P. D. Jones, V. da Costa Bechtold, A. C. M. Beljaars, P. W. Kallberg, S. Saarinen, S. M. Uppala, P. Viterbo, and N. Wedi. 2004. "Comparison of Trends and Low-Frequency Variability in CRU, ERA-40, and NCEP/NCAR Analyses of Surface Air Temperature." *Journal of Geophysical Research* 109: D24115. doi:10.1029/2004JD005306.

Sitch, S., A. D. McGuire, J. Kimball, N. Gedney, J. Gamon, R. Engstrom, A. Wolf, Q. Zhuang, J. Clein, and K. C. McDonald. 2007. "Assessing the Carbon Balance of Circumpolar Arctic Tundra Using Remote Sensing and Process Modeling." *Ecological Applications* 17 (1): 213–234. doi:10.1890/1051-0761(2007)017[0213:ATCBOC]2.0.CO;2.

Suzuki, R., H. Kobayashi, N. Delbart, J. Asanuma, and T. Hiyama. 2011. "NDVI Responses to the Forest Canopy and Floor from Spring to Summer Observed by Airborne Spectrometer in Eastern Siberia." *Remote Sensing of Environment* 115: 3615–3624. doi:10.1016/j.rse.2011.08.022.

Tanja, S., F. Berninger, T. Vesala, T. Markkanen, P. Hari, A. Makela, H. Ilvesniemi, H. Hanninen, E. Nikinmaa, T. Huttula, T. Laurila, M. Aurela, A. Grelle, A. Lindroth, A. Arneth, O. Shibistova, and J. Lloyd. 2003. "Air Temperature Triggers the Recovery of Evergreen Boreal Forest Photosynthesis in Spring." *Global Change Biology* 9: 1410–1426. doi:10.1046/j.1365-2486.2003.00597.x.

Tape, K. D., M. Hallinger, J. M. Welker, and R. W. Ruess. 2012. "Landscape Heterogeneity of Shrub Expansion in Arctic Alaska." *Ecosystems (New York, N.Y.)* 15: 711–724. doi:10.1007/s10021-012-9540-4.

Tucker, C. J., J. E. Pinzon, M. E. Brown, D. Slayback, E. W. Pak, R. Mahoney, E. Vermote, and N. El. Saleous. 2005. "An Extended AVHRR 8-Km NDVI Data Set Compatible with MODIS and SPOT Vegetation NDVI Data." *International Journal of Remote Sensing* 26 (20): 4485–4498. doi:10.1080/01431160500168686.

Tucker, C. J., J. R. G. Townshend, and T. E. Goff. 1985. "African Land Cover Classification Using Satellite Data." *Science* 227: 369–375. doi:10.1126/science.227.4685.369.

Vadrevu, K. P., and Y. Choi. 2011. "Wavelet Analysis of Airborne CO_2 Measurements and Related Meteorological Parameters over Heterogeneous Landscapes." *Atmospheric Research* 102: 77–90. doi:10.1016/j.atmosres.2011.06.008.

Verbyla, D. 2008. "The Greening and Browning of Alaska Based on 1982–2003 Satellite Data." *Global Ecology and Biogeography* 17: 547–555. doi:10.1111/j.1466-8238.2008.00396.x.

Wang, X., S. Piao, P. Ciais, J. Li, P. Friedlingstein, C. Koven, and A. Chen. 2011. "Spring Temperature Change and Its Implication in the Change of Vegetation Growth in North America from 1982 to 2006." *Proceedings of the National Academy of Sciences of the United States of America* 108 (4): 1240–1245. doi:10.1073/pnas.1014425108.

Winton, M. 2006. "Amplified Arctic Climate Change: What Does Surface Albedo Feedback Have to Do with It?" *Geophysical Research Letters* 33: L03701.

Xu, L., R. B. Myneni, F. S. Chapin III, T. V. Callaghan, J. E. Pinzon, C. J. Tucker, Z. Zhu, J. Bi, P. Ciais, H. Tommervik, E. S. Euskirchen, B. C. Forbes, S. L. Piao, B. T. Anderson, S. Ganguly, R. R. Nemani, S. J. Goetz, P. S. A. Beck, A. G. Bunn, C. Cao, and J. C. Stroeve. 2013. "Temperature and Vegetation Seasonality Diminishment over Northern Lands." *Nature Climate Change* 3: 581–586. doi:10.1038/nclimate1836.

Xueref-Remy, I., P. Bousquet, C. Carouge, L. Rivier, N. Viovy, and P. Ciais. 2010. "Variability and Budget of CO_2 in Europe: Analysis of the CAATER Airborne Campaigns – Part 2: Comparison of CO_2 Vertical Variability and Fluxes from Observations and A Modeling Framework." *Atmospheric Chemistry and Physics Discussions* 10: 4271–4304. doi:10.5194/acpd-10-4271-2010.

Yi, S., A. D. McGuire, J. Harden, E. Kasischke, K. Manies, L. Hinzman, A. Liljedahl, J. Randerson, H. Liu, V. Romanovsky, S. Marchenko, and Y. Kim. 2009. "Interactions between Soil Thermal and Hydrological Dynamics in the Response of Alaska Ecosystems to Fire Disturbance." *Journal of Geophysical Research* 114: G02015. doi:10.1029/2008JG000841.

Yi, Y., J. S. Kimball, L. A. Jones, R. H. Reichle, R. Nemani, and H. Margolis. 2013. "Recent Climate and Fire Disturbance Impacts on Boreal and Arctic Ecosystem Productivity Estimated Using a Satellite-Based Terrestrial Carbon Flux Model." *Journal of Geophysical Research: Biogeosciences*, 118: 1–17. doi:10.1002/jgrg.20053.

Yue, S., P. Pilon, and G. Cavadias. 2002. "Power of the Mann-Kendall and Spearman's Rho Tests for Detecting Monotonic Trends in Hydrological Series." *Journal of Hydrology* 259: 254–271. doi:10.1016/S0022-1694(01)00594-7.

Zhang, K., J. S. Kimball, E. H. Hogg, M. Zhao, W. C. Oechel, J. J. Cassano, and S. W. Running. 2008. "Satellite-Based Model Detection of Recent Climate-Driven Changes in Northern High-Latitude Vegetation Productivity." *Journal of Geophysical Research* 113: G03033.

Zhang, K., J. S. Kimball, Y. Kim, and K. C. McDonald. 2011. "Changing Freeze-Thaw Seasons in Northern High Latitudes and Associated Influences on Evapotranspiration." *Hydrological Processes* 25 (26): 4142–4151.

Zhang, K., J. S. Kimball, R. R. Nemani, and S. W. Running. 2010. "A Continuous Satellite-Derived Global Record of Land Surface Evapotranspiration from 1983 to 2006." *Water Resources Research* 46: W09522. doi:10.1029/2009WR008800.

Zhao, T., L. Zhang, L. Jiang, S. Zhao, L. Chai, and R. Jin. 2011. "A New Soil Freeze/Thaw Discriminant Algorithm Using AMSR-E Passive Microwave Imagery." *Hydrological Processes* 25: 1704–1716. doi:10.1002/hyp.7930.

Zimov, S. A., E. A. G. Schuur, and F. S. Chapin III. 2006. "Permafrost and the Global Carbon Budget." *Science* 312: 1612–1613. doi:10.1126/science.1128908.